

Diquark mass and quark-diquark potential by lattice QCD using an extended HAL QCD method with a static quark.

Kai-Wen Kelvin-Lee^{a,*} and Noriyoshi Ishii^a

^a*Research Center for Nuclear Physics (RCNP), University of Osaka,
10-1 Mihogaoka, Ibaraki, Osaka 567-0047*

E-mail: kelvin@rcnp.osaka-u.ac.jp, ishiin@rcnp.osaka-u.ac.jp

We will calculate the diquark mass together with the quark-diquark potential. We apply an extended HAL QCD potential method to a baryonic system made up from a static quark and a diquark. Numerical calculations are performed by employing 2+1 flavor QCD gauge configurations generated by CP-PACS and JLQCD Collaborations on a $16^3 \times 32$ lattice with $a^{-1} \approx 1.6$ GeV. To improve the statistical noise in the propagators of the static quark, the HYP smearing is employed on the gauge links. Two-point correlators of quark-diquark baryonic system are then computed to obtain their ground-state energies where various types of diquarks are considered (eg: scalar diquark, axial-vector diquark etc). We apply an extended HAL QCD method on a baryonic system made up from a scalar diquark and a static quark to study the scalar diquark mass and the quark-diquark potential. In order to determine the diquark mass self-consistently in this HAL QCD method, we demand that the baryonic spectrum in the p-wave sector obtained from the two-point correlators should be reproduced by the potential obtained from the baryonic system in the s-wave sector. We obtain the scalar diquark mass of roughly $(2/3)m_N$, i.e., twice the naïve estimates of a constituent quark mass together with the quark-diquark potential of Cornell type (Coulomb + linear).

*The 21st International Conference on Hadron Spectroscopy and Structure (HADRON2025)
27 - 31 March, 2025
Osaka University, Japan*

*Speaker

1. Introduction

Diquarks are hypothesized to be fundamental building blocks of hadrons and are believed to play a significant role in various QCD phenomena [1]. A diquark consists of two quarks, and the decomposition $\mathbf{3}_c \otimes \mathbf{3}_c = \bar{\mathbf{3}}_c \oplus \mathbf{6}_c$ indicates that diquarks necessarily carry a non-neutral color charge. Among the possible diquark configurations, the so-called “good” diquark—namely, the scalar diquark with quantum numbers $J^P = 0^+$, isospin $I = 0$, and color $\bar{\mathbf{3}}_c$ —is expected to be the most significant. This configuration is considered the lightest diquark, as it is energetically favored by both the color-magnetic interaction in the quark model and the instanton-induced interaction [2–5]. At high baryon number densities, such scalar diquarks are predicted to condense in the QCD vacuum, leading to spontaneous breaking of color SU(3) symmetry and the emergence of a new phase known as color superconductivity.

Despite their theoretical importance, experimental investigation of diquarks remains extremely challenging due to QCD color confinement, which prevents the observation of isolated diquarks. First-principles studies using lattice QCD are therefore essential for probing diquark properties. However, lattice QCD studies of diquarks are themselves complicated by color confinement, which renders standard techniques developed for color-singlet hadrons ineffective. For example, the conventional approach of extracting hadron masses via exponential fits to temporal two-point correlators is not justified for diquarks, as their correlators do not exhibit bound-state poles in momentum space (see Sec. 60.6.3 of Ref. [6]).

Nevertheless, several lattice QCD studies have attempted to investigate diquark masses over the years, and they can be broadly categorized into the following three approaches:

1. Applying single-exponential fits to diquark two-point correlators in the Landau gauge [7–9].
2. Introducing a static quark to neutralize the color charge and evaluating gauge-invariant quark-diquark two-point correlators to extract diquark mass differences [10–13].
3. Interpreting the diquark mass as a parameter in a non-relativistic quark-diquark potential model and employing an extended HAL QCD method to extract both the mass and the potential [14–16].

In category 1, stable plateaus are observed in the Landau-gauge correlators, which are then fitted with a single exponential to estimate the diquark mass. However, the absence of a true bound-state pole in the correlators is not adequately addressed. Category 2 maintains color SU(3) gauge invariance by introducing a static quark and constructing baryon-like systems composed of the static quark and a diquark. Diquark mass differences are estimated from the energy differences between such baryonic systems. However, these estimates do not explicitly account for the interaction energy between the diquark and the static quark, which introduces uncertainty in the extracted diquark mass differences. (Besides mass differences, this approach also yields interesting insights into the spatial extent of diquarks.)

In category 3, an extended HAL QCD method is used to construct a quark-diquark model in which the diquark mass appears as a parameter. Here, Λ_c and Σ_c baryons are treated as bound states of a charm quark and a diquark. This approach avoids the issue of missing bound-state poles in diquark two-point correlators. However, the extracted diquark mass is sensitive to the input charm

quark mass, which introduces ambiguity. It should be noted that the determination of the charm quark mass itself is also not unique.

In the present work, we improve upon the above approaches by employing an extended HAL QCD method, with a static quark replacing the charm quark in the Λ_c -like system. This modification eliminates the ambiguity associated with the charm quark mass encountered in category 3. Moreover, by combining the static quark with the HAL QCD method, we also address the limitations of category 2. Specifically, the interaction energy between the static quark and the diquark can be explicitly separated from the total energy of the baryonic system, thereby resolving the uncertainty in the extracted diquark mass differences.

In this paper, we present our results for the mass of the scalar diquark as well as the quark-diquark potential, obtained using this improved framework.

2. Formalism

Since diquarks carry color charge $\bar{\mathbf{3}}_c$, their two-point correlators do not exhibit physical poles in momentum space due to color confinement [6]. Consequently, direct extraction of diquark masses from temporal two-point correlators via a single-exponential fit should be avoided. To overcome this issue, we follow the same strategy as in category 3, attempting to eliminate the ambiguity associated with the charm quark mass by replacing the charm quark with a static quark of infinite mass.

We first note that the angular momentum of our baryonic states can essentially be specified by the orbital angular momentum L of the diquark relative to the static quark. This is justified for two reasons: First, we restrict ourselves to scalar diquarks in this study. Second, the spin of the static quark is completely decoupled and factorized from the rest of the baryonic system, since the static quark corresponds to the heavy quark limit of the charm quark (Heavy Quark Spin Symmetry). Accordingly, the baryonic state can be denoted as $|B(L)\rangle$, where L is the orbital angular momentum between the diquark and the static quark.

We now consider the equal-time Nambu–Bethe–Salpeter (NBS) wavefunction of the baryonic system composed of a static quark and a diquark:

$$\psi_L(\mathbf{r}) \equiv \langle 0 | D_c(\mathbf{x}) Q_c(\mathbf{y}) | B(L) \rangle, \quad \mathbf{r} \equiv \mathbf{x} - \mathbf{y}, \quad (1)$$

where $Q_c(x)$ is the static quark field, and $D_c(x)$ is the composite scalar diquark field defined as

$$D_c(x) \equiv \epsilon_{abc} u_a^T(x) C \gamma_5 d_b(x), \quad (2)$$

with $C \equiv i\gamma^2\gamma^0$ being the charge conjugation matrix. We require that this NBS wavefunction satisfies the following Schrödinger equation:

$$\left(-\frac{\nabla^2}{2m_D} + \hat{V} \right) \psi_L(\mathbf{r}) = (\varepsilon_L - m_D) \psi_L(\mathbf{r}), \quad (3)$$

where ε_L denotes the total relativistic energy of the baryonic state $|B(L)\rangle$. Here, m_D is the diquark mass, which will be determined later by requiring consistency between the baryonic masses obtained from this model and those extracted from two-point correlators. The quantity $(\varepsilon_L - m_D)$

corresponds to the “binding energy” of the system. The operator \hat{V} represents the quark–diquark potential, which is derivatively expanded as $\hat{V} \simeq V_0(r) + O(\nabla)$, where $V_0(r)$ is the central (spin-independent) potential. Due to the scalar nature of the 0^+ diquark, the spin–spin and tensor interactions are absent. Moreover, because the spin of the static quark decouples, the spin–orbit interaction is also absent.

The equal-time NBS wavefunction is extracted from the quark–diquark four-point correlator. For positive time separations $t > 0$, our quark-diquark four-point correlator is arranged as

$$C(\mathbf{r}, t; t_{\text{src}}) \equiv \frac{1}{V} \sum_{\Delta} \langle 0 | D_c(\mathbf{r} + \Delta, t) Q_c(\Delta, t) \cdot \mathcal{J}^\dagger(t_{\text{src}}) | 0 \rangle \quad (4)$$

$$= \frac{1}{V} \sum_{\Delta} \sum_n \langle 0 | D_c(\mathbf{x} + \Delta, t) Q_c(\Delta, t) | n \rangle \langle n | \mathcal{J}^\dagger(t_{\text{src}}) | 0 \rangle \cdot e^{-E_n(t-t_{\text{src}})}, \quad (5)$$

where V is the spatial volume, and the sum over Δ projects to zero spatial momentum. The states $|n\rangle$ and energies E_n denote the n -th eigenstates and eigenvalues of the QCD Hamiltonian, respectively. $\mathcal{J}(t_{\text{src}})$ denotes the source operator. To enhance the overlap with the ground state, we examine the wall and the exponentially smeared sources with several smearing size.

To specify the source explicitly, we define $q_a(f, t) \equiv \sum_{\mathbf{x}} q_a(\mathbf{x}, t) f(\mathbf{x})$ for $q = u, d, Q$ with $f(\mathbf{x}) : \mathbb{R}^3 \rightarrow \mathbb{C}$. Then, $D_c(f, t) \equiv \epsilon_{abc} u_a^T(f, t) C \gamma_5 d_b(f, t)$, and the source operator is

$$\mathcal{J}(t) \equiv D_{c'}(f, t) Q_{c'}(f, t), \quad (6)$$

where we choose $f(\mathbf{x}) \equiv 1$ for the wall source and $f(\mathbf{x}) \equiv \exp(-|\mathbf{x}|/b)$ with $b = a, 2a, 3a$ for smearing sources, where a is the lattice spacing.

In the large- t limit, the four-point correlator is dominated by the ground state, and the S-wave NBS wavefunction $\psi_S(\mathbf{r})$ is obtained as

$$\psi_S(\mathbf{r}) \propto C(\mathbf{r}, t; t_{\text{src}}) \quad \text{for large } t. \quad (7)$$

Since we use wall and smeared sources, the extracted NBS wavefunctions correspond to the S-wave.

We define the “prepotential” $\tilde{V}_0(\mathbf{r})$ from the NBS wavefunction as

$$\tilde{V}_0(\mathbf{r}) \equiv \frac{\nabla^2 \psi_S(\mathbf{r})}{\psi_S(\mathbf{r})}. \quad (8)$$

Applying the Schrödinger equation (3) to the S-wave, we obtain

$$\tilde{V}_0(\mathbf{r}) = 2m_D [V_0(\mathbf{r}) + m_D - \varepsilon_S], \quad (9)$$

where $\varepsilon_S \equiv \varepsilon_{L=S}$.

Using the prepotential, we rewrite the Schrödinger equation for the P-wave as the following “pre-Schrödinger” equation:

$$\left(-\nabla^2 + \tilde{V}_0(r) \right) \psi_P(\mathbf{r}) = \Delta \tilde{E} \psi_P(\mathbf{r}), \quad (10)$$

where $\varepsilon_P \equiv \varepsilon_{L=P}$ and $\Delta \tilde{E} \equiv 2m_D(\varepsilon_P - \varepsilon_S)$.

We determine the diquark mass m_D by requiring consistency between the baryonic masses obtained from the two-point correlators and those from the Schrödinger equation. This is done by solving Eq. (10) using the prepotential $\tilde{V}_0(\mathbf{r})$ in the P-wave sector to extract $\Delta\tilde{E}$. Then, m_D is determined by

$$m_D = \frac{\Delta\tilde{E}}{2(\varepsilon_P - \varepsilon_S)}, \quad (11)$$

using the values of ε_P and ε_S extracted from two-point correlators. Once m_D is obtained, the quark-diquark potential is reconstructed as

$$V_0(r) = \frac{1}{2m_D} \tilde{V}_0(r) + m_D - \varepsilon_S. \quad (12)$$

3. Numerical Results and Discussion

3.1 Lattice QCD Setup

We perform our lattice QCD calculations using the $2 + 1$ flavor ($ud + s$) gauge configurations generated by CP-PACS and JLQCD Collaborations [17]. This ensemble consists of 454 configurations on a $16^3 \times 32$ lattice, generated with the renormalization-group improved (Iwasaki) gauge action at $\beta = 6/g^2 = 1.83$, combined with a nonperturbatively $O(a)$ -improved (clover) quark action at $\kappa_{ud} = \kappa_s = 0.13710$ (the SU(3) flavor-symmetric point) using $C_{\text{SW}} = 1.761$. This setup corresponds to a lattice spacing of $a \approx 0.1209(16)$ fm ($a^{-1} \approx 1.632$ GeV), spatial extent $La \approx 1.934$ fm, pion mass $m_\pi \approx 1014$ MeV, and nucleon mass $m_N \approx 2026$ MeV [18].

Before calculating the two-point and four-point correlators, Coulomb gauge fixing is applied. Hypercubic (HYP) smearing [19] is then applied to the gauge links to construct the static quark propagators (Wilson lines), thereby reducing statistical fluctuations. We use both wall sources and exponentially smeared sources for the light-quark and static-quark propagators. To further suppress statistical noise, we exploit translational symmetry in the temporal direction by averaging over 16 source points: $t_{\text{src}}/a = 0, 2, 4, \dots, 30$. Rotational symmetry (cubic group) and combined time-reversal and charge-conjugation symmetries are also used to reduce noise. Statistical errors are estimated using the jackknife method with a bin size of 10 configurations.

3.2 Effective Mass Differences

We consider two-point correlators of baryonic systems composed of a diquark and a static quark:

$$G_\Gamma(t) \equiv \left\langle J_\Gamma(\mathbf{x}, t) J_\Gamma^\dagger(\mathbf{x}, 0) \right\rangle, \quad (13)$$

where $J_\Gamma(x) \equiv \epsilon_{abc} (u_a^T(x) C \Gamma d_b(x)) Q_c(x)$ denotes the interpolating operator for the baryonic state, and $\Gamma = 1, \gamma_\mu, \gamma_5, \gamma_5 \gamma_\mu, \sigma_{\mu\nu}$.

The static quark propagator is replaced by a temporal Wilson line:

$$S_{\text{stat}}(\mathbf{x}_2, t_2; \mathbf{x}_1, t_1) = \delta^3(\mathbf{x}_2 - \mathbf{x}_1) \left(\frac{1 + \gamma_0}{2} \right) \left[\prod_{t=t_1}^{t_2-a} U_4(\mathbf{x}_1, t) \right]^\dagger \quad (14)$$

for $t_2 > t_1$, where the factor $\exp(-m_Q(t_2 - t_1))$ is dropped with $m_Q = \infty$ being the mass of the static quark. The effective mass is defined in the standard way:

$$m_{C\Gamma}(t) \equiv a^{-1} \log [G_\Gamma(t)/G_\Gamma(t+a)]. \quad (15)$$

Following Ref. [10], we define the effective mass difference as

$$\Delta m_{C\Gamma}(t) \equiv m_{C\Gamma}(t) - m_{C\gamma_5}(t), \quad (16)$$

which is the effective mass difference between the baryonic states with diquark channels $C\Gamma$ and $C\gamma_5$. $\Delta m_{C\Gamma}(t)$ is a gauge invariant quantity, which can serve as a good estimate of the mass difference between the two diquark channels according to the additive diquark model of heavy baryons (see Sect. 8.4 of Ref. [20]).

Figure 1 shows the effective mass differences obtained from wall-source propagators. Our

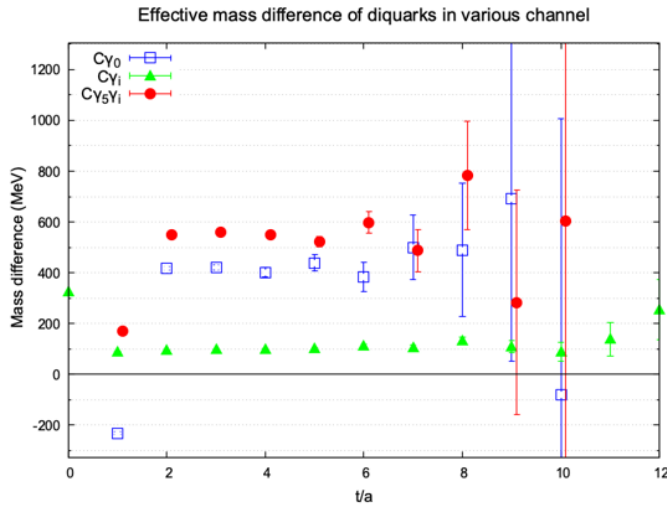


Figure 1: Effective mass differences $\Delta m_{C\Gamma}$ for baryonic states corresponding to various diquark channels, computed from wall-sourced two-point correlators.

results are consistent with those in Ref. [10]. In the positive parity sector, the ‘‘bad’’ axial-vector diquark is heavier than the ‘‘good’’ scalar diquark. Negative-parity states are heavier than positive-parity states. We also observe that, in both parity sectors, vector diquarks tend to be heavier than scalar diquarks.

We emphasize that our interpretation of the 1^- state differs from that in Ref. [10]. Whereas Ref. [10] treated this state as a 1^- diquark in S-wave, we interpret it as a 0^+ diquark in P-wave. Our interpretation is supported by phenomenological studies, where λ -mode excitations are favored over ρ -mode excitations [21]. This reinterpretation is crucial for applying the HAL QCD method presented later.

3.3 NBS Wavefunction and Prepotential from the Four-Point Correlator

The normalized four-point correlators $\tilde{C}(\mathbf{r}, t) \equiv C(\mathbf{r}, t)/C(\mathbf{0}, t)$ are plotted in Fig. 2 as a function of $r = |\mathbf{r}|$ for fixed time slices $t = 2, 4, 6, \dots$. We use three types of sources: SRC01 ($f(\mathbf{r}) \equiv$

$\exp(-|\mathbf{r}|/a)$, SRC03 ($\exp(-|\mathbf{r}|/(3a))$), and SRC08 (wall source). For all three, convergence is roughly achieved at $t/a \gtrsim 10$, with SRC01 showing the fastest convergence. We thus adopt SRC01 for subsequent analysis.

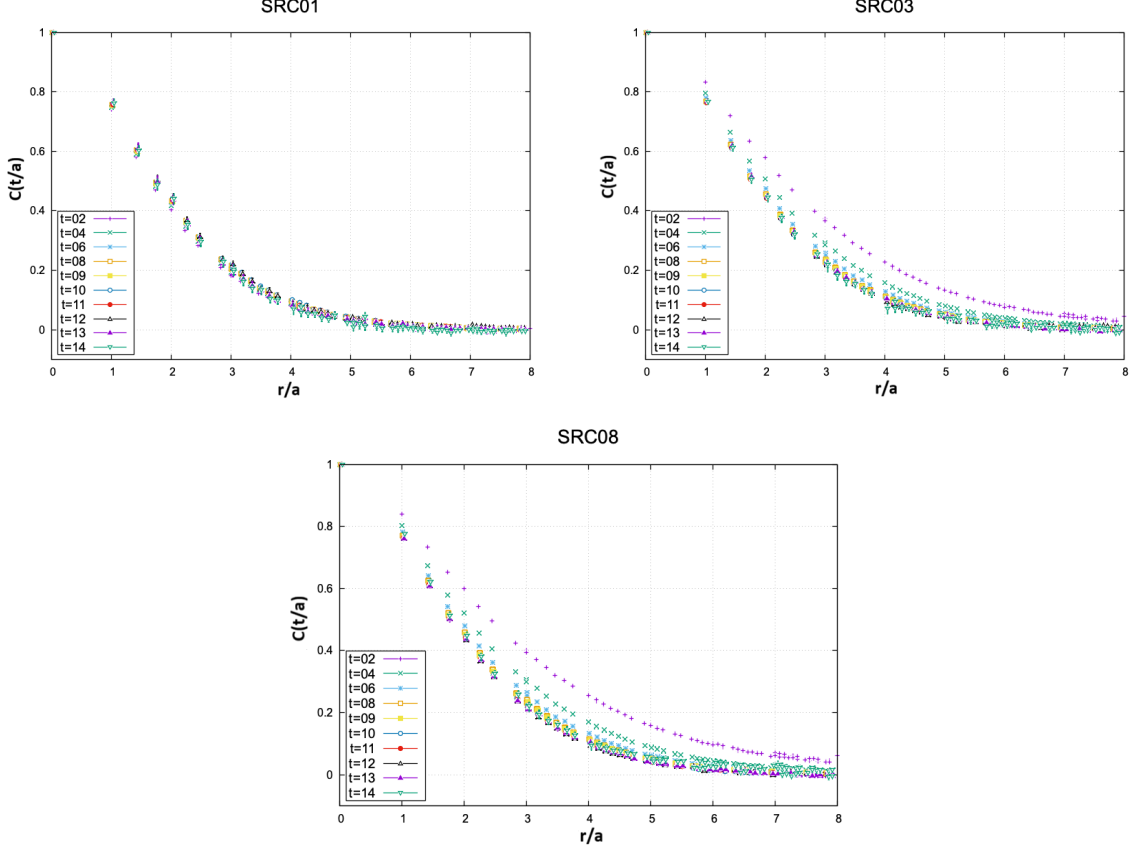


Figure 2: Convergence behavior of four-point correlators using three types of sources. SRC01 and SRC03 denote exponentially smeared sources with $f(r) = \exp(-r)$ and $\exp(-r/3)$, respectively (in lattice units). SRC08 denotes the wall source. Convergence rate: SRC01 > SRC03 > SRC08.

3.4 Prepotential

Figure 3 shows the prepotentials $\tilde{V}_0(\mathbf{r})$ computed using SRC01 for various time slices. Convergence is observed at $t/a \gtrsim 10$. We take the result at $t/a = 10$ as the converged prepotential, which we fit using a Cornell-type function:

$$\tilde{V}_0^{\text{fit}}(\mathbf{r}) = -\frac{A}{r} + Br + v_0.$$

3.5 Scalar Diquark Mass m_D and the Quark–Diquark Potential

We solve the pre-Schrödinger equation (10) in the P-wave sector using the fitted Cornell-type prepotential. The bound-state solution is obtained via the shooting method with the Dormand–Prince fifth-order Runge–Kutta (RK) algorithm [22].

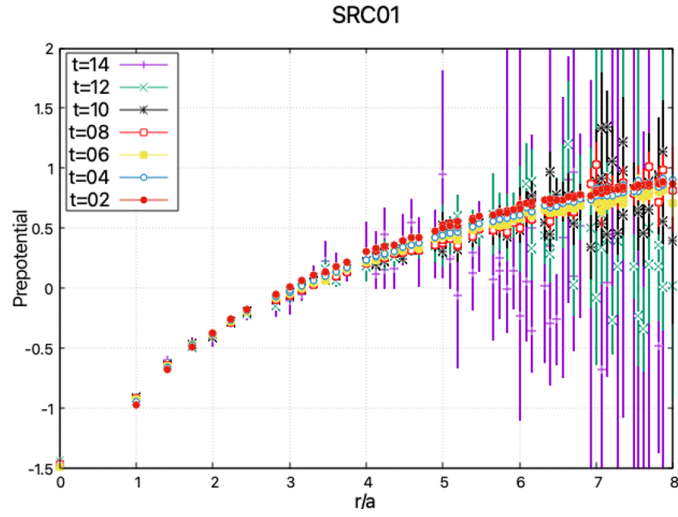


Figure 3: Prepotentials for $t/a = 2, 4, \dots, 14$ using SRC01.

Using Eq. (11) with the extracted $\Delta\tilde{E}$ and the effective energies ε_P and ε_S from the two-point correlators, we obtain the scalar diquark mass as

$$m_D \simeq 1.241 \text{ GeV}, \quad (17)$$

which is roughly consistent with the naive estimate based on constituent quark mass, i.e., $(2/3)m_N \simeq 1.35 \text{ GeV}$.

The quark-diquark potential is then obtained from Eq. (12), and is shown in Fig. 4.

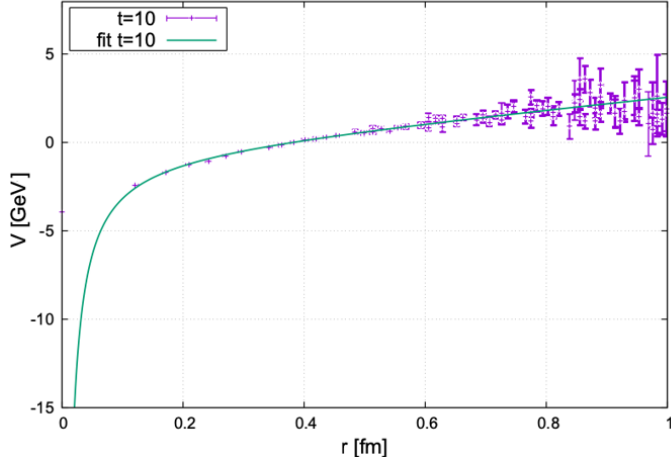


Figure 4: The quark-diquark potential.

Fitting this potential with the Cornell form $V_0(r) = -A/r + Br + v_0$ yields:

$$\begin{aligned} A &= 0.121(4) \text{ GeV} \cdot \text{fm}, \\ \sqrt{B} &= 510(5) \text{ MeV}, \\ v_0 &= 0.141(15) \text{ GeV}. \end{aligned}$$

We note that HYP smearing affects short-distance behavior ($r \lesssim 2a$), which impacts the Coulomb coefficient A . Our extracted string tension \sqrt{B} is slightly larger than the conventional value from the static quark–antiquark potential (~ 440 MeV) [23].

4. Conclusion and Future Outlook

We have presented a lattice QCD study of baryonic systems composed of a diquark and a static quark, aiming to determine the diquark mass and the quark–diquark potential. Our calculations are based on 2 + 1 flavor QCD gauge configurations generated by CP-PACS and JLQCD Collaborations on a $16^3 \times 32$ lattice.

Following Ref. [10], we computed the effective mass differences between two baryonic systems containing different diquarks. These mass differences provide gauge-invariant estimates of diquark mass differences under the additive diquark picture, and our results are consistent with those in Ref. [10].

To overcome the issue of the absence of a bound-state pole in diquark two-point correlators, we treated the diquark mass as a mass parameter within a quark–diquark model. We constructed this model by applying an extended HAL QCD potential method to baryonic systems composed of a scalar (“good”) diquark and a static quark. Since the static quark has infinite mass, our method avoids the ambiguity associated with the choice of charm quark mass in previous studies. The diquark mass was determined by imposing a consistency condition between the baryonic mass in the P-wave sector—obtained via the Schrödinger equation—and the baryonic mass extracted from two-point correlators. Our result for the scalar diquark mass is $m_D \simeq 1.241$ GeV, which is close to $2m_N/3 \simeq 1.35$, i.e., twice the naive estimate of the constituent quark mass.

Importantly, our method allows for explicit decomposition of the baryonic mass into the sum of the diquark mass and the quark–diquark interaction energy. While Ref. [10] interpreted mass differences between baryonic systems as diquark mass differences, our framework enables a direct and explicit determination of both the diquark mass and its mass differences from first principles.

We have also extracted the quark–diquark potential, which exhibits a Cornell-like behavior (Coulomb + linear confinement), with a string tension of $\sqrt{\sigma} = 510(5)$ MeV—slightly larger than the conventional value of ~ 440 MeV.

For future work, we plan to apply variational analysis with multiple source operators to improve the precisions of the diquark mass and the quark-diquark potentials. We will extend the present framework to the axial-vector channel to determine axial-vector diquark mass. We will investigate the dependence of the diquark masses and the quark-diquark potentials differences on the quark mass to make an extrapolation to the physical quark mass point.

Acknowledgments

Numerical calculations in this work were performed on the supercomputer SQUID at D3 Center of Osaka University, supported by the Research Center for Nuclear Physics (RCNP), Osaka University. We thank the CP-PACS and JLQCD Collaborations as well as the JLDG/ILDG for providing the 2 + 1 flavor QCD gauge configurations. We employed a modified version of the lattice QCD library Bridge++ to carry out our computations [24]. This work was supported by JSPS KAKENHI Grant Number JP21K03535. We acknowledge the support from the Ministry of Education, Culture, Sports, Science and Technology (MEXT) of Japan through the Japanese Government Scholarship.

References

- [1] R. L. Jaffe. Exotica. *Nucl. Phys. B Proc. Suppl.*, 142:343, 2005.
- [2] G. 't Hooft. *Physical Review D*, 14(12):3432–3450, 1976.
- [3] E.V. Shuryak. The role of instantons in quantum chromodynamics. *Nuclear Physics B*, 203(1):93–115, 1982.
- [4] T. Schäfer and E. V. Shuryak. Instantons in qcd. *70*(2):323–425, 1998.
- [5] Edward Shuryak and Ismail Zahed. A schematic model for pentaquarks based on diquarks. *Physics Letters B*, 589(1–2):21–27, 2004.
- [6] R.L. Workman et al PDG. Review of particle physics. *Progress of Theoretical and Experimental Physics*, 2022(8):083C01, 2022.
- [7] M. Hess, F. Karsch, E. Laermann, and I. Wetzorke. Diquark masses from lattice qcd. *Phys. Rev. D*, 58:111502, 1997.
- [8] R. Babich, N. Garron, C. Hoelbling, J. Howard, L. Lellouch, and C. Rebbi. Diquark correlations in baryons on the lattice with overlap quarks. *Phys. Rev. D*, 76:074021, 2007.
- [9] Y. Bi, Hao Cai, Y. Chen, M. Gong, Z. Liu, H.-X. Qiao, and Y.-B. Yang. Diquark mass differences from unquenched lattice qcd. *Chin. Phys. C*, 40:073106, 2016.
- [10] C. Alexandrou, Ph. de Forcrand, and B. Lucini. Evidence for diquarks in lattice qcd. *Phys. Rev. Lett.*, 97:222002, 2006.
- [11] A. Francis, P. de Forcrand, R. Lewis, and K. Maltman. Diquark properties from full qcd lattice simulations. *JHEP*, 05:062, 2022.
- [12] K. Orginos. Diquark properties from lattice qcd. In *PoS LAT2005*, page 054, 2006.
- [13] J. Green, J. Negele, M. Engelhardt, and P. Varilly. Spatial diquark correlations in a hadron. In *PoS LATTICE2010*, page 140, 2010.

- [14] N. Ishii K. Watanabe. Building diquark model from lattice qcd. *Few Body Syst.*, 23(3):45, 2021.
- [15] Kai Watanabe. Quark-diquark potential and diquark mass from lattice qcd. *Phys. Rev. D*, 105:074510, 2022.
- [16] S. Nishioka and N. Ishii. Axialvector diquark mass and quark-diquark potential in Σ_c . *PoS (LATTICE2024)*, 305, 2025.
- [17] T. Ishikawa et al. Light-quark masses from unquenched lattice qcd. *Phys. Rev. D*, 78:011502(R), 2008.
- [18] T. Inoue, N. Ishii, S. Aoki, T. Doi, T. Hatsuda, Y. Ikeda, K. Murano, H. Nemura, and K. Sasaki. Baryon-baryon interactions in the flavor su(3) limit from full qcd simulations on the lattice. *Progress of Theoretical Physics*, 124(4):591–603, 2010.
- [19] Anna Hasenfratz and Francesco Knechtli. Flavor symmetry and the static potential with hypercubic blocking. *Physical Review D*, 64(3), 2001.
- [20] W. Weise U. Vogl. The nambu and jona-lasinio model: Its implications for hadrons and nuclei. *Progress in Particle and Nuclear Physics*, 27:195–272, 1991.
- [21] Hideko Nagahiro, Shigehiro Yasui, Atsushi Hosaka, Makoto Oka, and Hiroyuki Noumi. Structure of charmed baryons studied by pionic decays. *Physical Review D*, 95(1), 2017.
- [22] William H. Press. *Numerical recipes in C++: The Art of Scientific Computing*. Cambridge Univ. Press India, 2007.
- [23] K. Schilling and G. S. Bali. The static quark-antiquark-potential: A “classical” experiment on the connection machine cm-2. *International Journal of Modern Physics C*, 04(06):1167–1177, 1993.
- [24] author = S. Ueda, S. Aoki, T. Aoyama, K. Kanaya, H. Matsufuru, S. Motoki, Y. Namekawa, H. Nemura, Y. Taniguchi, and N. Ukita. Development of an object oriented lattice qcd code ‘bridge++’. *J. Phys. Conf. Ser.* 523 012046., (523), 2014.